Balloon-borne FIREBall-2 ultraviolet spectrograph stray light control based on nonsequential reverse modeling of on-sky data

Trenton Brendel[a,*] **Aafaque Khan**[a,b] **Simran Agarwal**[a,b] **Heejoo Choi**[a] **Daewook Kim**[a,b] **Erika Hamden**[b] **Vincent Picouet**[c] **D. Christopher Martin**[d] **Bruno Milliard**[e] **David Schiminovich**[c] **Shouleh Nikzad**[f] **Jean Evrard**[g] **Nicolas Bray**[g] **Johan Montel**[g] **Keri Hoadley**[h] **Drew M. Miles**[d] **Gillian Kyne**[f] **Jessica Li**[d] **Zeren Lin**[c] **Haeun Chung**[b] **Philippe Balard**[e] **Patrick Blanchard**[e] **Marty Crabill**[d] **Charles-Antoine Chevrier**[g] **Alain Peus**[g] **Ignacio Cevallos-Aleman**[c] **Olivia Jones**[b] **Harrison Bradley**[b] **Naz Ipek Kerkeser**[b] **Matthew Werneken**[c] **Didier Vibert**[e] **Nicole Melso**[b] and **David Valls-Gabaud**[i]

[a]University of Arizona, Wyant College of Optical Sciences, Tucson, Arizona, United States
[b]University of Arizona, Steward Observatory, Tucson, Arizona, United States
[c]Columbia University, Astronomy Department, New York, New York, United States
[d]California Institute of Technology, Division of Physics, Math, and Astronomy, Pasadena, California, United States
[e]Laboratoire d'Astrophysique de Marseille, Marseille, France
[f]Jet Propulsion Laboratory, California Institute of Technology, Pasadena, California, United States
[g]Centre national d'études spatiales, Toulouse, France
[h]University of Iowa, Department of Physics and Astronomy, Iowa City, Iowa, United States
[i]Observatoire de Paris LERMA, Paris, France

Abstract. We present a comprehensive stray light analysis and mitigation strategy for the FIREBall-2 ultraviolet balloon telescope. Using nonsequential optical modeling, we identified the most problematic stray light paths, which impacted telescope performance during the 2018 flight campaign. After confirming the correspondence between the simulation results and post-flight calibration measurements of stray light contributions, a system of baffles was designed to minimize stray light contamination. The baffles were fabricated and coated to maximize stray light collection ability. Once completed, the baffles will be integrated into FIREBall-2 and tested for performance preceding the upcoming flight campaign. Given our analysis results, we anticipate a substantial reduction in the effects of stray light. [DOI: 10.1117/1.JATIS.8.4.048001]

Keywords: stray light analysis; optomechanical design; nonsequential ray tracing.

Paper 22060G received Jun. 10, 2022; accepted for publication Nov. 4, 2022; published online Nov. 25, 2022.

1 Introduction

The faint intergalactic-medium redshifted emission balloon (FIREBall-2) is a balloon-borne, ultraviolet (UV) multiobject spectrograph (MOS) designed to observe faint emission from the halos of galaxies. FIREBall-2 is an international collaboration between the United States (Caltech, JPL, Columbia University, University of Arizona, and University of Iowa) and France (Centre National d'Études Spatiales and Laboratoire d'Astrophysique de Marseille). This suborbital astronomical balloon telescope, jointly funded by NASA and CNES, is designed

*Address all correspondence to Trenton Brendel, tbrendel@optics.arizona.edu

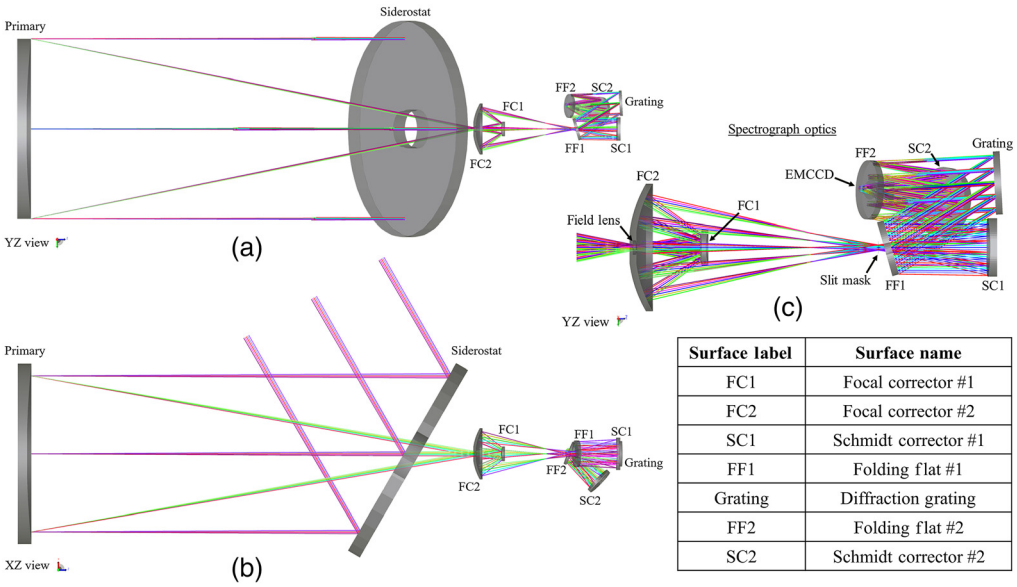

Surface label	Surface name
FC1	Focal corrector #1
FC2	Focal corrector #2
SC1	Schmidt corrector #1
FF1	Folding flat #1
Grating	Diffraction grating
FF2	Folding flat #2
SC2	Schmidt corrector #2

Fig. 1 The FIREBall-2 spectrograph nominal optical configuration, oriented on its side. The surface labels in the table appear in sequential optical order. (a) YZ view of the optical layout; (b) XZ view of the optical layout; and (c) closeup YZ view of the spectrograph optics inside of the vacuum tank.

to explore the forefront of modern extra-galactic astronomy through the discovery and mapping of faint emission from the intergalactic medium and circumgalactic medium (CGM) around moderate-redshift galaxies ($z \sim 0.7$). FIREBall-2 helps to improve our understanding of the vast diversity of nearby galaxies through the study of galactic feedback, including matter and energy outflows. By exploiting a convenient balloon window between the atmospheric O_2 and O_3 absorption bands above 37 km altitude, FIREBall-2 observes line emission in the $\lambda = 1980$ to 2130 Å band. FIREBall-2 is uniquely positioned as the only MOS to have ever flown on a balloon and the only UV MOS currently operating.

The FIREBall optical design is described in more detail in Hamden et al.[1] and includes multiple components, as illustrated in Fig. 1. All optical surface labels are defined in the included table. A 1.2-m diameter siderostat mirror provides field selection and angular altitude control, directing light to a 1-m parabolic primary mirror. This primary focuses light through a hole in the siderostat and into the spectrograph tank, which is kept at vacuum to allow the CCD detector to cool to −105°C. A small field correcting lens is located at the top of the spectrograph tank, where light from the parabola comes to an intermediate focus. Inside the spectrograph tank, there are two field correcting mirrors, referred to as FC1 and FC2, which improve the field of view from 10 arc sec (in the original FIREBall[2]) to allow 4.5 arc sec resolution over the 30-arc min field of view. At the field corrector focus is a slit mask carousel, which allows one of up to nine masks to be selected for use in flight. The masks are curved to match the spherical focal plane. Each mask is custom laser cut for a particular field of view. After the mask, the spectrograph optics consist of two spherical Schmidt mirrors (SC1 and SC2), a diffraction grating, and two folding flats (FF1 and FF2) for compactness. The detector is a Teledyne e2v CCD201-20, an EMCCD for photon counting.[3] This complex system requires a sophisticated baffling strategy, which we describe in Secs. 3 and 4.

2 Stray Light in the 2018 Fireball-2 Flight

2.1 *Flight Characteristics*

FIREBall-2 last flew on September 22, 2018, from Fort Sumner, New Mexico, USA, during the fall Columbia Scientific Balloon Facility campaign. Unfortunately, the flight suffered an

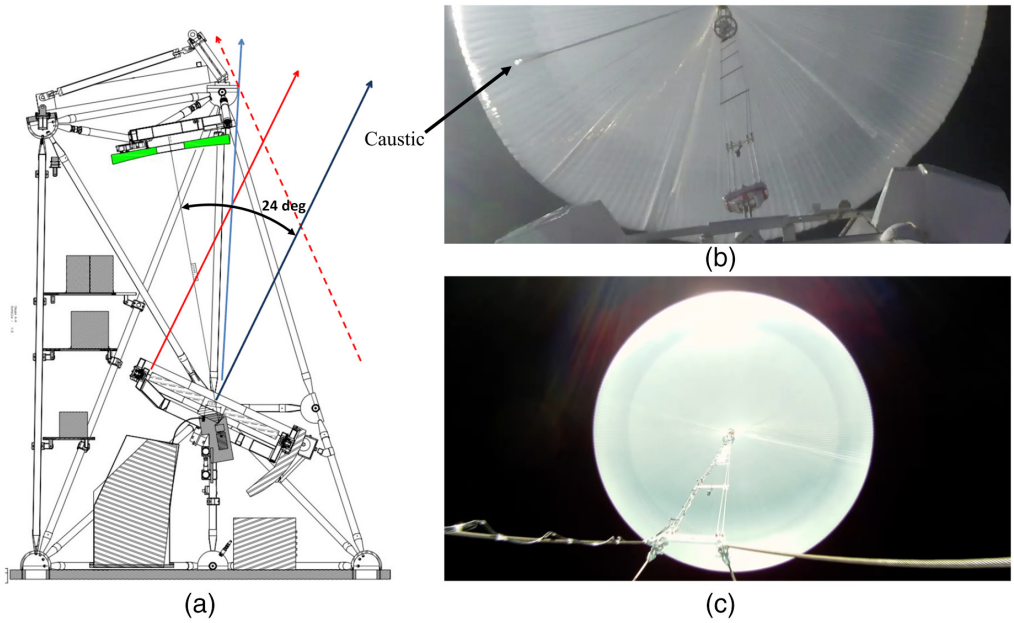

Fig. 2 Damaged balloon was the primary contributor to the excessive stray light exhibited during the 2018 flight. (a) Schematic depicting the ± 24 deg view angle of the siderostat onto the partially deflated balloon. (b) Upward view from the gondola looking toward the damaged balloon. (c) Example of an undamaged stratospheric balloon. Image courtesy of NASA Wallops.

anomaly, significantly impacting the science goals. A hole in the balloon, discovered when the balloon reached float altitude of 128,000 ft, caused the balloon to descend after only 3 h at the float altitude. The payload remained above the minimum allowable science altitude for about 1 h after astronomical twilight. The atmospheric transmission for the FIREBall-2 bandpass is highly dependent on altitude, with about a 10% reduction for every 3 km of altitude lost. As the altitude decreased over the course of the flight, the UV throughput dropped sharply, negatively impacting the ability to observe faint targets as planned.

2.2 *Stray Light Problem*

During the flight, FIREBall-2 suffered from severe stray light contamination, which compromised the observational effectiveness of the spectrograph. The cause of observed stray light is primarily attributed to moonlight scattered or reflected from the partially deflated balloon directly into the spectrograph, as demonstrated in Fig. 2. This problem was exacerbated by launch timing, which forced the flight to take place during a full moon, drastically increasing the stray light background.

After the abrupt touchdown of FIREBall-2 and an inventory of damage sustained, the team conducted postflight calibrations, during which the primary stray light paths were confirmed.[4,5] Based on the results of the postflight calibration, a preliminary baffling strategy was proposed. We present the work done since to implement the proposed strategy and expand the scope and effectiveness of stray light control measures.

3 Stray Light Analysis of a UV Balloon Telescope

3.1 *Stray Light Signature*

The optical performance of FIREBall-2 was substantially degraded by various stray light signatures. The main source of stray light was determined to be moonlight scattered and reflected off of the partially deflated balloon overhead, as shown in Fig. 3. A hole caused the balloon shape to deviate from the nominal spherical shape to a teardrop shape, which directed and focused light

(a) (b)

Fig. 3 (a) Damaged balloon was bathed in bright lunar illumination during the 2018 FIREBall-2 flight campaign. (b) Resultant lunar stray light produced a veiling glare on the detector.

into the telescope and directly into the spectrograph tank. The orientation and brightness of the full moon exacerbated the problem, scattering visible light into a direct path from the top of the spectrograph tank onto the back surface of the PCB mount, which then reflected onto the detector surface. This stray light path was not controlled for in optical analyses and is believed to be the most problematic source of background light reducing detector performance. The scattered light background was $\sim$100$\times$ more than expected. The photon counting capability of the EMCCD detector was not used during flight because of an excess of scattered light, resulting in higher than expected count rates on the detector ($>$ 1/event/pixel/frame). This corresponds to a flux of 0.59 e^-/pixel, or 40 e^-/h, during science observations.

In addition to the elevated background levels, flashes of light were observed at certain orientations where moonlight was focused directly into the system by conical sections of the lower part of the teardrop-shaped balloon. These flashes were $\sim$2 to 3 times higher in flux than the expected background or CGM signal. The flash was so severe that any images containing flashes were discarded from analysis. There is also a possibility that some of these flashes were caused by specular reflections from the support structure holding the primary mirror and the gondola doors.

More recently, a glint was discovered on the edge of the first Schmidt corrector mirror (SC1). Sneak paths through the medium bench assembly between the first folding flat (FF1) and the second folding flat (FF2) illuminate the rough edge of the mirror, scattering light up toward the detector through the hole in FF2.

3.2 *Nonsequential Optical Modeling*

To correct the stray light contamination problem, FIREBall-2 was modeled in detail using Zemax OpticStudio®. By incorporating all of the optical features specified in the sequential optical model, a nonsequential model was constructed which closely matched the optical performance of the nominal system. By comparing the full-field point spread function of the sequential and nonsequential models, we demonstrated the near equivalence in performance between the two models, as demonstrated in Fig. 4.

Apertures were modeled accurately, along with the as-built optical surface specifications. Positioning and orientation of all optical components was carefully checked and rechecked to ensure the validity of results derived using the model. Mechanical objects were added as necessary to accurately characterize the possible stray light paths. A balance was struck between detail and simplicity to optimize ray tracing performance. All critical limiting apertures were included and surfaces known to be involved in producing the stray light were considered.

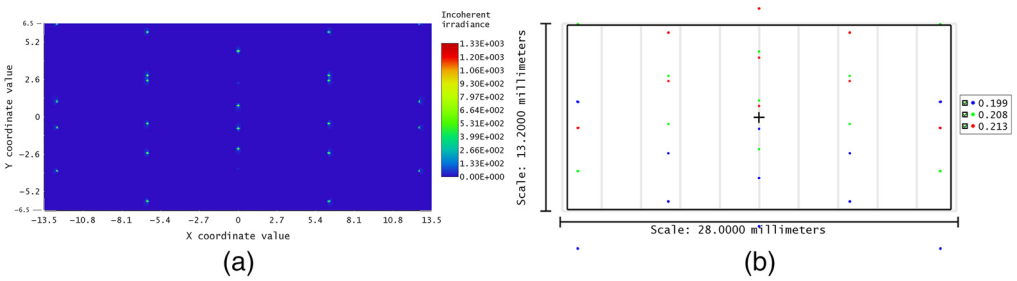

Fig. 4 (a) Detector irradiance distribution produced with the nonsequential optical model. (b) Footprint diagram generated with the sequential optical model.

Scattering properties were applied to critical surfaces using both built-in and measured scatter distributions.

Stray light baffles from the 2018 flight campaign were included in the original design. As new baffles were designed and tested, they were added in one by one to replace the original baffles. Figure 5 illustrates the changes made within the spectrograph between the 2018 flight configuration and the present configuration. Figure 5(a) includes: the original conical baffle located beneath FC1; the undersized pupil plane baffle fixed to rods and positioned above the slit mask; the foil grating mask attached to the diffraction grating (which was destroyed in 2018); and the tongue baffle protruding beneath FF2. Figure 5(b) includes: the remanufactured conical baffle beneath FC1; the significantly enlarged pupil plane baffle; the newly added glint baffle between SC1 and the grating; the updated grating mask fixed to the grating blank with tabs; the improved tongue baffle attached to FF2; and the new detector baffle bonded to the rear of FF2. Performance with and without the proposed baffle solutions was characterized qualitatively and quantitatively.

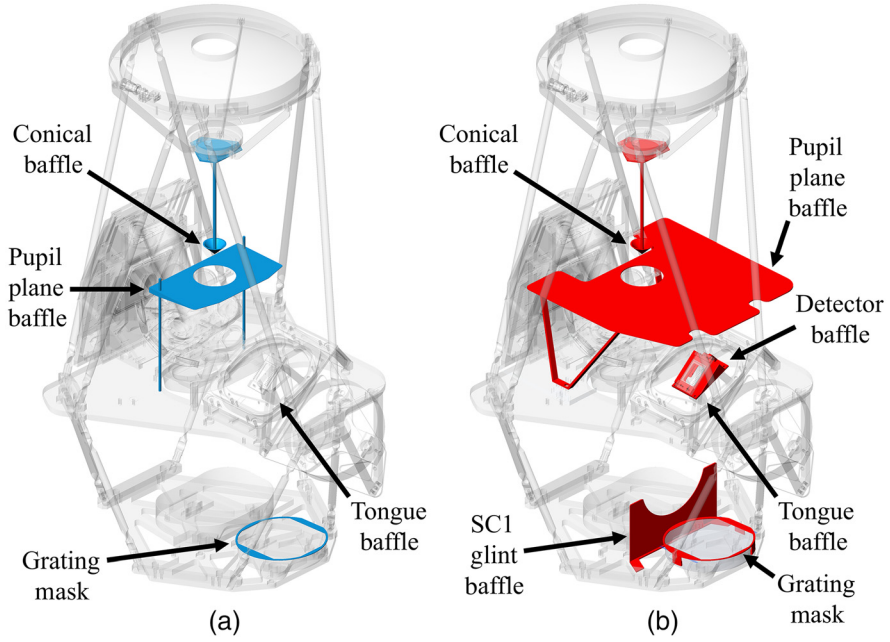

Fig. 5 (a) FIREBall-2 spectrograph configuration from the 2018 flight campaign with baffles highlighted in blue. (b) Updated FIREBall-2 spectrograph with newly added baffles highlighted in red. The conical baffle beneath FC1 was been rebuilt, the pupil plane baffle was significantly increased in size, the SC1 glint baffle was added, the grating mask was remade, and the detector baffle was added behind FF2.

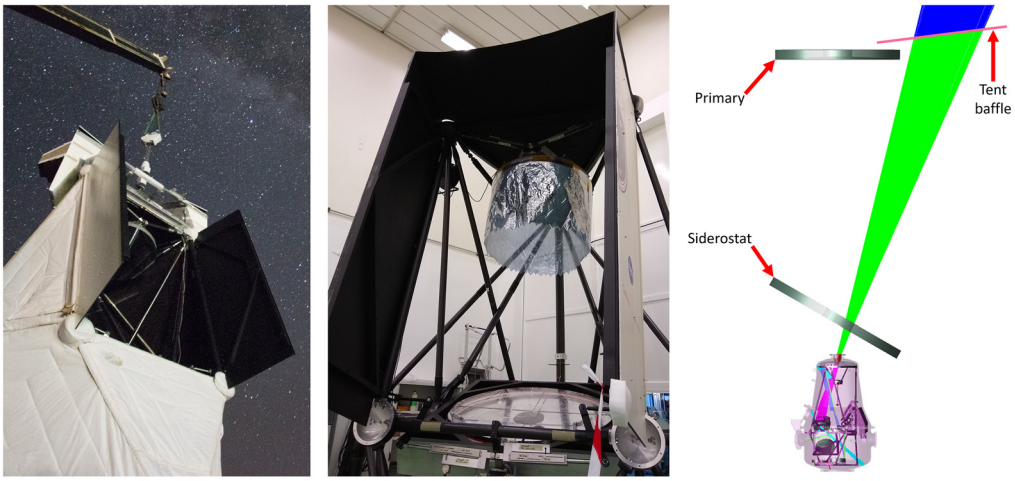

Fig. 6 (a) Upward view of the FIREBall-2 gondola doors open, allowing light to enter the gondola structure from above. (b) Tent baffle situated atop the gondola doors blocks balloon-emitted light from entering the spectrograph tank through the siderostat hole. (c) Simulation of the tent baffle blocking stray light emanating from the balloon (blue rays from balloon turn green when blocked).

4 Stray Light Mitigation Strategy

A comprehensive system of baffles was designed and fabricated for installation on FIREBall-2, highlighted in Fig. 5. By considering all previously identified stray light paths as well as new paths discovered during detailed analysis, baffles were implemented at locations best suited to block any and all unwanted light from making its way to the sensitive EMCCD detector.

4.1 *Tent Baffle*

The first baffle introduced on the FIREBall-2 telescope following the 2018 flight campaign was the tent baffle. As the most problematic stray light path was quickly determined to originate at the balloon, the tent baffle was the logical first choice for implementation. Attached to the top of the gondola doors, the tent baffle extends 50 cm from the top of the gondola and allows unobscured observations up to a 65-deg elevation angle. Made out of black, flexible fabric, this baffle is deployed upon opening of the gondola doors, as demonstrated in Fig. 6. With the primary source of stray light being traced to the conical underside of the balloon, this baffle is poised to significantly reduce the stray light background by preventing light emanating from the illuminated balloon from passing through the hole in the siderostat and entering the vacuum tank through the field lens. This particular stray light path has been identified as one of the most damaging contributions given the substantial fraction of energy that may be deposited in the region nearby the detector.

4.2 *Conical Baffle*

One of the stray light paths previously identified involves double and triple bounce ray paths on the field corrector mirrors at the top of the spectrograph tank. A conical baffle positioned below the first focal corrector mirror (FC1) was used to capture ray bundles following these unwanted paths and redirect them away from the mask/guider system, as shown in Fig. 7. The original baffle was fabricated with a thin sheet of black anodized aluminum and included a shiny edge exposed to the unwanted irradiance. This baffle was damaged beyond repair during the 2018 flight campaign.

The conical baffle was redesigned to improve its durability and its effectiveness at capturing stray light. The walls of the cone were thickened and diameter of the opening aperture slightly expanded to contain more of the offending ray paths at the edge of the focal corrector optics. The

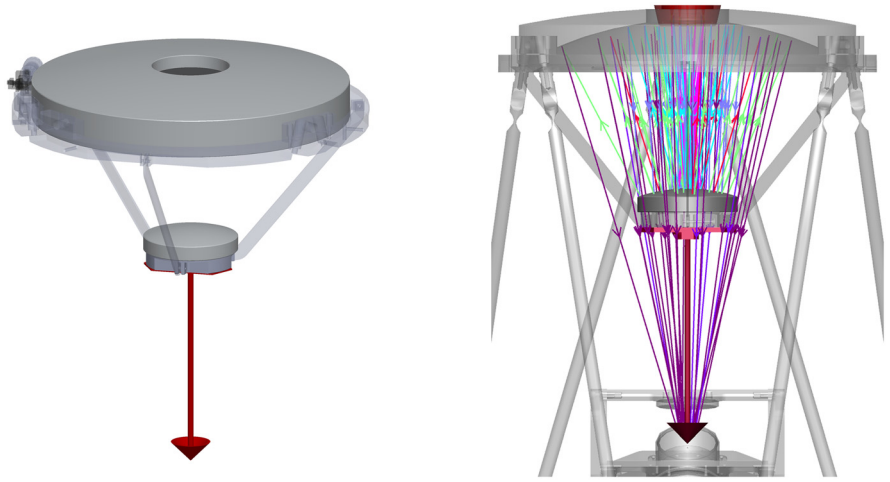

Fig. 7 (a) Conical baffle (red) situated beneath the focal corrector optics catches double and triple bounce paths between FC1 and FC2, as indicated at right by the per-segment coloration of ray paths. (b) Each ray path sequentially evolving through violet, cyan, periwinkle, green, and purple constitute a double bounce path which is captured by the baffle.

new baffle is coated with Avian-S to minimize scattering off of surfaces inclined toward the detector and maximize light trapping.

4.3 *Pupil Plane Baffle*

One of the most significant stray light paths identified during the 2018 postflight calibrations involved light propagating from the top of the spectrograph tank onto surfaces in close proximity to the detector. The 2018 flight hardware included a baffle situated near the intermediate pupil plane between the focal corrector optics and the field mask, implemented to permit passage of only light which is contained within the nominal pupil ellipse. A proposal was made to extend the outer diameter of this pupil plane baffle to block any stray light which might follow the unwanted ray paths described above. The redesigned baffle is shown at right in Fig. 8 alongside the old baffle. The outer diameter of the baffle has been extended to effectively separate the upper part of the spectrograph tank from the lower part, with the pupil plane as the dividing interface. This new design isolates the lower region of the tank from receiving any unwanted light and greatly increases the chances of a successful observational campaign.

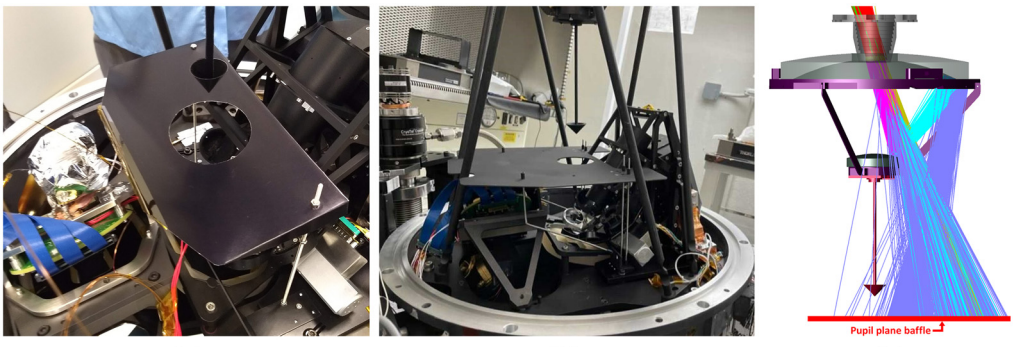

Fig. 8 (a) Old pupil plane diaphragm was constructed of thin, metal foil, and mounted on threaded posts. (b) New pupil plane diaphragm is fabricated from sheet metal and mounted to the guider camera bench with six aluminum gussets. (c) New pupil plane diaphragm with significantly improved coverage isolates the upper part of the spectrograph tank from the lower bench.

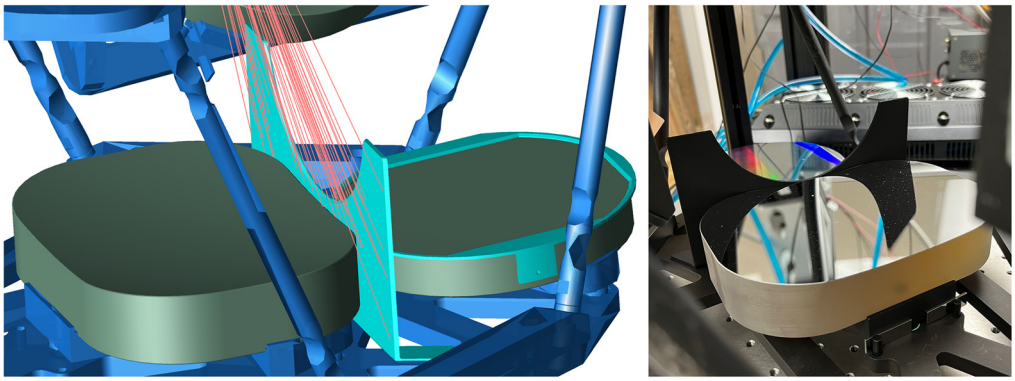

(a) (b)

Fig. 9 (a) SC1 glint baffle blocking rays which illuminate the unpolished, chamfered edge of the SC1 mirror. This mirror edge scatters light directly toward the detector, as observed in the laboratory. (b) Installed baffle, coated with Avian-S, mounted to the bottom bench in between the SC1 mirror and the colorfully illuminated grating.

4.4 *SC1 Glint Baffle*

An unexpected stray light path was discovered by observation during lab testing. Glints of light reflecting off of the edge of the SC1 mirror after traversing a sneak path through the medium bench assembly between the FF1 and FF2 mirrors have the potential to send light toward the detector and increase the background. A barrier attached to the bottom of the spectrograph tank obscuring the edge of the SC from illuminating downstream optics prevents these potential ray paths from reaching the detector, as demonstrated in Fig. 9. The barrier is coated with Avian-S to maximize absorption.

4.5 *Grating Mask*

The mask affixed to the grating, blocking the region outside the clear aperture of the elliptical grating surface, was badly damaged during the 2018 flight campaign. For the upcoming flight campaign, a new mask was designed and fabricated. With an emphasis on robustness and stray light mitigation, this new mask shown in Fig. 10 presents significant improvements over the previous mask, which was fabricated with a thin foil taped to the grating surface. Our new mounting solution using tabs and adhesive to fix the mask to the outer edge of the grating blank will reduce the risk of damaging the fragile grating surface. Considering the close proximity of

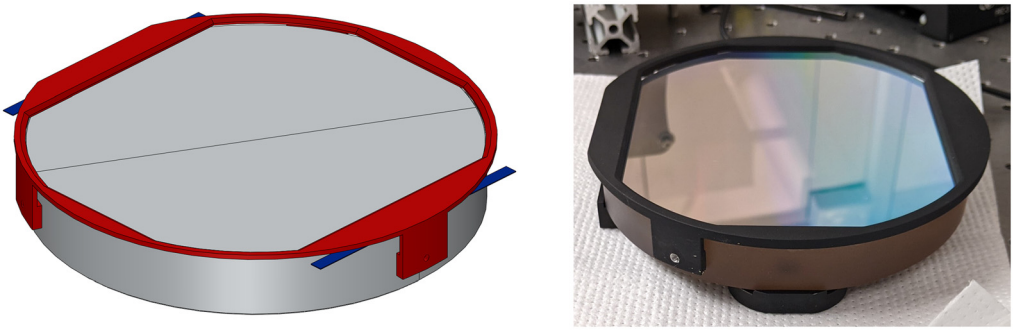

(a) (b)

Fig. 10 (a) Grating mask with fixed to the outer face of the grating blank. Spacers shown in blue are used during mask installation to prevent damage to the grating surface and then removed after the adhesive sets. (b) Coated grating mask during a fit check on the flight grating. The mounting mechanism was later updated as shown in Sec. 6.6.

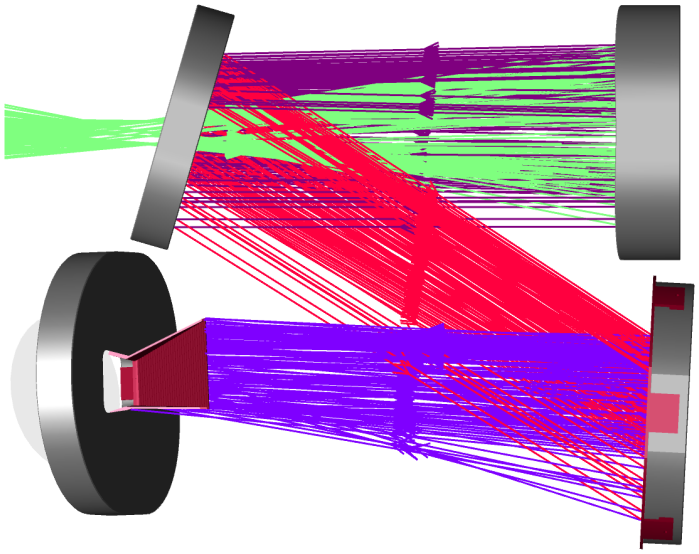

Fig. 11 Unwanted direct-to-detector ray paths are blocked by the tongue baffle. The tongue baffle also blocks light just outside of the waveband of interest.

the grating surface to the detector plane, the performance of this mask is crucial for mitigating stray light.

4.6 *Tongue Baffle Improvements*

A baffle attached to the FF2 mirror and extending down toward the grating was incorporated into the 2018 flight hardware. The baffle was included for two reasons: (1) to prevent light from proceeding directly from the diffraction grating onto the detector without first reflecting off of FF2 and SC2, illustrated in Fig. 11 and (2) to block diffraction orders outside of the sole +1-order for which the system was designed. However, the baffle was designed with a smooth top surface oriented at a high angle of incidence to the chord connecting the grating and the detector, allowing for a significant portion of light contacting the black anodized surface to specularly reflect or scatter onto the detector plane.

The tongue baffle, shown in Fig. 12, was redesigned with threading on the top face of the tongue surface to prevent unwanted light from reflecting and scattering into the vicinity of the detector. The thread orientation is orthogonal to the plane of incidence of the majority of rays

(a) (b) (c)

Fig. 12 (a) Tongue baffle upon receipt from ProtoLabs postmanufacturing. (b) Baffle was later coated with Avian-S optical black at Caltech to minimize scattering near the detector. (c) Tongue baffle installed onto the FF2 mirror hole.

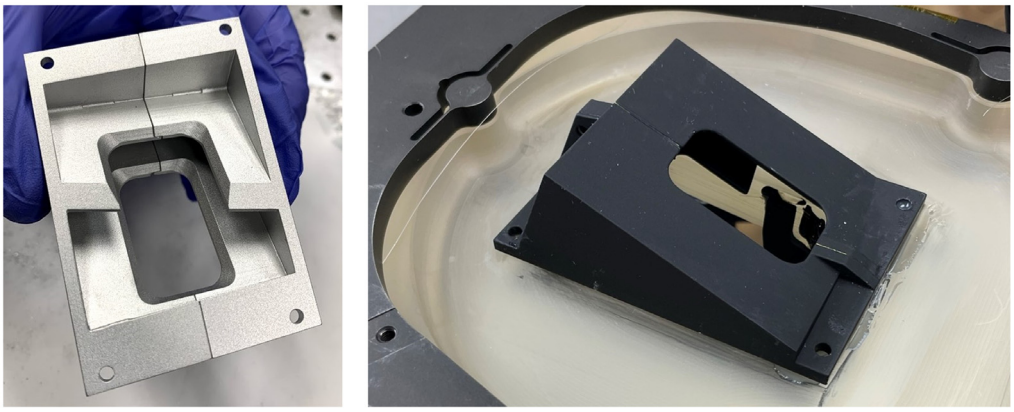

(a) (b)

Fig. 13 (a) The front view of the ProtoLabs-fabricated detector baffle with respect to the sequential optical path. The vanes are designed to redirect rays away from the detector plane and capture unwanted light scattered from the FF2 central hole into the intervane cavity. (b) The baffle was later coated with Avian-S at Caltech and transported to Columbia University for integration into the FIREBall-2 spectrograph. The image shows the baffle fixed to the backplane of the FF2 mirror.

intercepting the front face after diffracting, thereby redirecting light away at a steep angle. The baffle was coated with Avian-S polyurethane coating chosen for its success in aerospace applications, its low outgassing in high vacuum environments, and its durability.

4.7 *Detector Baffle*

To mitigate the risk of light scattering from the unpolished backplane of FF2 or the inner walls of the center hole in mirror FF2 from interacting with the detector, the detector baffle shown in Fig. 13 was developed. It is believed that sneak paths allowed stray light to illuminate the backplane of FF2 and scatter onto the detector during the 2018 flight campaign. The baffle encapsulates the ray cones across the field converging onto the detector plane and fills the gap between the inclined detector package and the back of FF2. The space between the FF2 backplane and the detector plane was identified as the most likely source of much of the scattered stray light observed in 2018. Vanes trap and redirect unwanted light in spectrograph tank away from the focal plane. The baffle is coated in Avian-S to reduce scattering. The vanes were designed geometrically, using principles described in Ref. 6. Proximity to the detector and the high risk of near-to-detector stray light renders this baffle critical for mission success.

5 Effectiveness of Implementation

To ensure the effectiveness of the stray light mitigation plans, verification testing was conducted for each baffle. Nonsequential ray tracing with and without each baffle showed marked improvements in the stray light rejection with the inclusion of the baffles. Nonsequential analysis results were compared with on-sky images highlighting stray light features. A comparative study of the distribution of stray light across the detector plane was used to quantitatively analyze the validity of the developed model.

Figure 14 demonstrates the effectiveness of the baffle implementation at mitigating stray light. The image at left depicts a typical stray light distribution from the 2018 FIREBall-2 flight campaign. The most notable features are the density of irradiance in the bottom right diagonal of the detector plane, which is replicated in center left figure containing detector irradiance results from a nonsequential ray tracing analysis. The source of stray light in this simulation comes from a radial source spanning 13.5 deg to 24 deg from vertical, modeled as an analog to lunar radiation redirected from a fully illuminated balloon above FIREBall-2. This source configuration was identified as the most problematic stray light contribution during the 2018 flight and was therefore the most pressing issue to overcome.

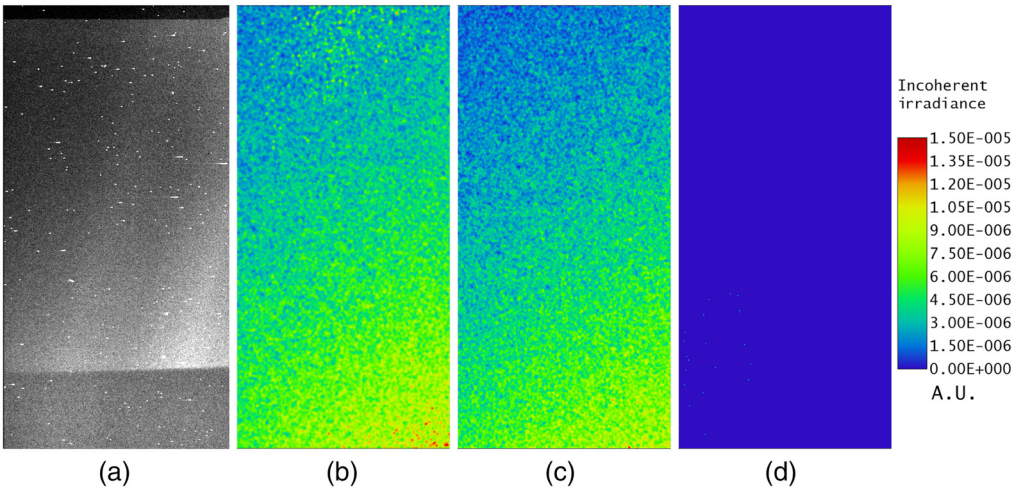

Fig. 14 (a) On-sky image of stray light observed during the 2018 flight campaign. (b) Detector irradiance from a nonsequential ray trace simulating the stray light distribution from on-sky with no baffles installed. (c) Marginal reduction in stray light with the inclusion of the detector baffle. (d) Nearly complete mitigation of stray light with both the detector baffle and the pupil plane baffle included. The inclusion of the tent baffle alone is also able to affect this sharp reduction in stray light.

When the detector baffle is added to the optical model, stray light in the upper portion of the detector is reduced, but there is still substantial irradiance streaming into the detector at high angles after scattering off of the rear surface of the FF2 mirror. It should be noted that the detector baffle was designed with substantial margin between the detector plane and the mechanical surface to minimize the risk of interference, and this margin reduces the baffle's ability to block high-angle stray light. However, when the pupil plane baffle is included, the baffle designed specifically to block the direct paths to the detector, which were identified in 2019, the stray light from the source described above is entirely blocked, as shown in Fig. 14(c). Moreover, if only the tent baffle is included, all stray light from this source configuration is blocked, as shown in Fig. 14(d). Redundancy in baffling solutions is essential to promote mission success, as there is a small risk of tearing the tent baffle or other possible failure modes.

6 Baffle Integration

A plan for integrating the system of baffles developed for FIREBall-2 was developed by Aafaque Khan and Simran Agarwal in conjunction with colleagues at Columbia University. Multiple baffles were fixed in place using 3M EC 2216 B/A Scotch-Weld Epoxy Adhesive, while others were bolted onto the upper and lower spectrograph benches. The epoxy was mixed by volume with syringes and degassed with a vacuum pump in a bell jar.

The biggest challenge of the integration process was that the spectrograph optics had already been aligned, meaning that baffles had to be installed *in situ* with the mirrors in place. This was particularly problematic for the grating mask, but the team made effective use of protective tents to prevent optics from being damaged while baffles were positioned.

6.1 *Tongue Baffle Integration*

Before installation of the tongue baffle, leftover epoxy on FF2 from the 2018 campaign required that parts of the baffle tabs be removed manually, as chipping off epoxy could have damaged the mirror. The baffle was sent back to Caltech for recoating after the interfering regions were removed. The tongue baffle was fixed to the inner hole of the FF2 mirror with adhesive and a 3D-printed "casquette" tool to press the tabs onto the mirror edge, as illustrated in Fig. 15. The baffle tabs first catch the edge of the mirror during by-hand installation, then the casquette tool

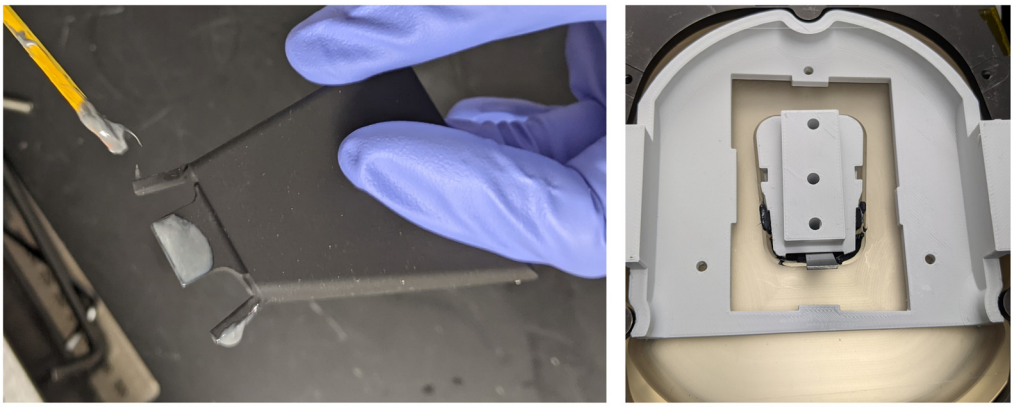

(a) (b)

Fig. 15 (a) View of the bottom side of tongue baffle with epoxy being applied to the mounting tabs. (b) Rear view of the casquette tool inserted into the FF2 hole and pressed onto the baffle tabs. The 3D-printed tool ensures that the baffle is positioned and oriented correctly.

precisely positions and orients the baffle as pressure is applied. A shim and kapton tape were inserted at the edge of the tool to ensure a tight fit during epoxy curing.

6.2 *Detector Baffle Integration*

Next, the detector baffle was installed onto the back of the FF2 mirror using a 3D-printed jig and shims for positioning as shown in Fig. 16. With the jig placed on FF2 and adhesive applied to bottom of the baffle, the baffle was pressed onto FF2 and shims were applied to the top and bottom along with kapton tape to fix the baffle in place during epoxy curing. Once the epoxy cured, the jig was removed and the detector assembly was installed for a fit check.

6.3 *Thermal Analysis of Detector Baffle*

There was a mild concern that the proximity of the detector baffle to the cold detector and copper cold clamp connected to the detector, as shown in Fig. 16(b), could cool the baffle via radiative heat transfer. This cooling could induce thermal gradients in the FF2 mirror and potentially stress the adhesive bonding contacts past the point of failure.

To ensure that these thermal gradients did not pose a mission critical risk, we conducted a thermal simulation involving the Zerodur FF2 mirror, the detector baffle, and the radiating copper detector clamp. The detector clamp has the largest view factor to the detector baffle, so this was the only cold surface used in the model. Direct thermal contact was assumed between the baffle and FF2, as the thickness of the adhesive bond would have an insignificant effect on steady

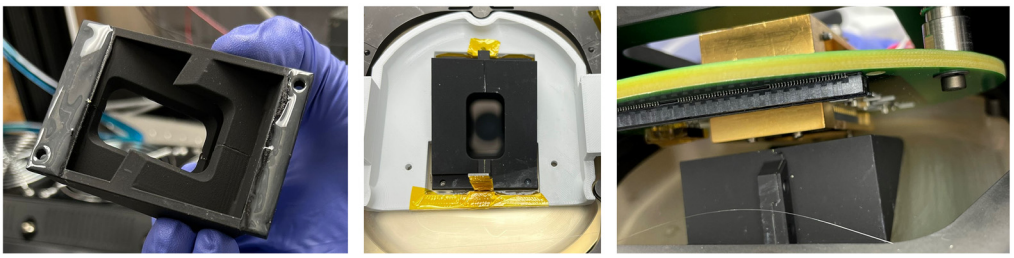

(a) (b) (c)

Fig. 16 Detector baffle (a) with epoxy on the bottom and (b) installed onto the backplane of FF2. The 3D-printed jig for baffle alignment was removed after the epoxy cured. (c) View showing the proximity of copper detector clamp to the detector baffle.

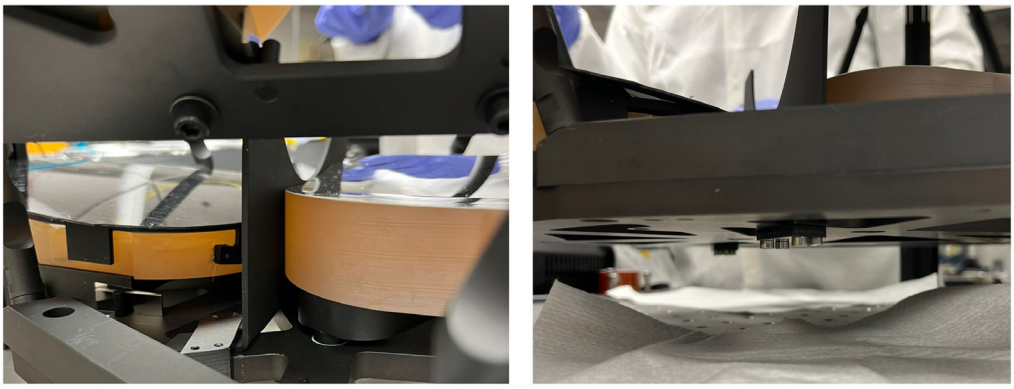

(a) (b)

Fig. 17 (a) Side view of the SC1 baffle mounted onto the bottom bench. (b) Underside view showing the mounting components under the bottom bench.

state thermal gradients. Various cases for mirror temperature boundary conditions and emissivity of the 110-K copper clamp were used in the model.

By analyzing the radiative transfer from the 110-K clamp to the detector baffle, the worst case scenario indicates that a thermal gradient of no >0.1 K from the coldest to the hottest spot on the baffle. We inferred that the high thermal mass of the mirror and the high conductivity and low thermal mass of the baffle average out the temperature. With these findings, we successfully confirmed that radiative transfer does not pose any risk of inducing failure in the baffle bond.

6.4 *SC1 Baffle Integration*

The SC1 glint baffle was bolted to the bottom bench of the spectrograph. Originally, the plan was to fix this sheet of metal in place with adhesive, but the team reconsidered this decision and decided to implement a clamping mechanism instead. Figure 17 shows a side view and an underside view of the mechanical clamping mechanism used to fix the baffle in place between SC1 and the grating.

6.5 *Conical Baffle Integration*

The conical baffle was one of the simplest baffles to install. Three threaded holes in the FC1 mounting ring on the field corrector assembly were used to install the baffle in 2018, and these same holes were for this installation. The baffle, coated with Avian-S, hangs beneath the field corrector optics as shown in Fig. 18.

6.6 *Grating Mask Integration*

The grating mask posed significant challenges during integration, not the least of which was the tight space into which it had to be installed. Originally, the mask was to be installed with three simple tabs contacting the outer edge of the blank. However, there was a mismatch between the size of the actual grating blank and the grating blank in the FIREBall-2 CAD model. This mismatch left too great a gap between the tabs and the edge of the blank for the adhesive to hold.

As such, a mounting method was developed by the team that used three additional clamping bars to which the original mounting tabs were attached. The new mounting solution is demonstrated in Fig. 19, where mounting clamps are bonded to the grating blank and the mask tabs are bolted onto these clamps.

6.7 *Pupil Plane Baffle Integration*

The pupil plane baffle is the last baffle to be installed. The baffle was mounted using a system of vertical gussets, metal rods attached to the mask guider bench atop the spectrograph medium

Fig. 18 The conical baffle is fastened onto the FC1 mounting ring and sits beneath the field corrector assembly.

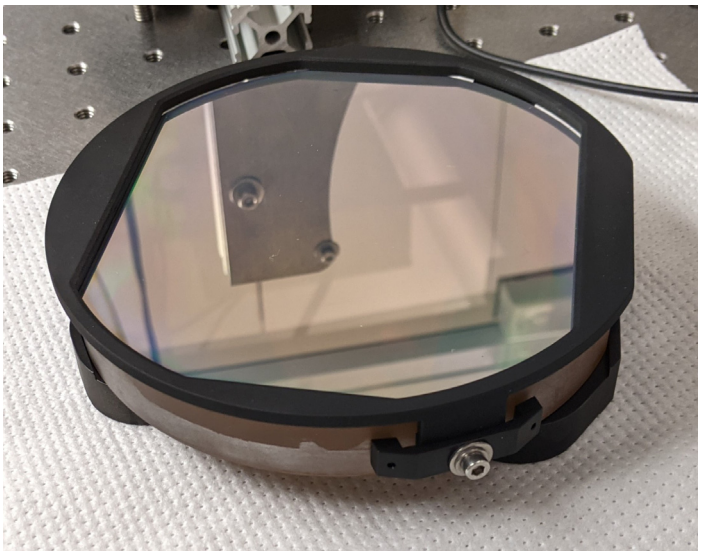

Fig. 19 The grating mask is attached to the grating blank through a set of three bonded clamps to which the mask tabs are bolted.

bench. Thin rods are used for mounting because of tight constraints on added mass. Structural support is provided almost entirely by four gussets, whereas two extra gussets are included to prevent flapping of thin metal sheet. A fit check of the baffle and a demonstration of the mounting scheme are shown in Fig. 20.

7 Conclusion

We have developed and implemented a stray light mitigation system on the FIREBall-2 UV balloon telescope. Comprehensive stray light analysis via nonsequential optical modeling, paired

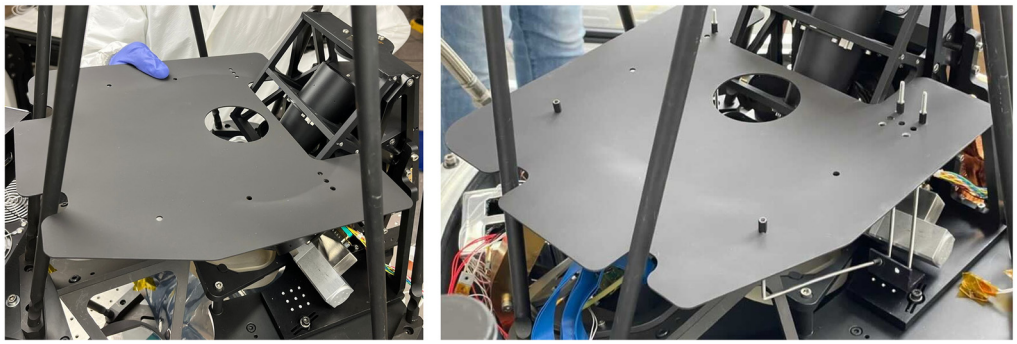

(a) (b)

Fig. 20 (a) The pupil plane baffle positioned above the spectrograph medium bench during a fit check. (b) The installed pupil plane baffle after detector shimming. Thin rods are used to hold the pupil plane baffle in place.

with on-sky stray light images enabled a unique and effective strategy for providing a comprehensive solution. Baffles were designed and fabricated and are planned for integration onto the telescope in the near future. With the proposed system of baffles, the next FIREBall-2 flight campaign will exhibit considerable improvements in stray light rejection and maximize scientific impact.

Acknowledgments

This project was funded primarily by the NASA APRA Program for suborbital missions which funds the US portion of FIREBall-2 (Award No. 80NSSC20K0262). FIREBall-2 is a collaboration between NASA, CNES, LAM, Caltech, Columbia, JPL, UIowa, and UArizona. The FIREBall-2 collaboration would like to thank the Columbia Scientific Ballooning Facility and Balloon Program Office (BPO/NASA) for their support during the 2022 campaign in Ft. Sumner, NM.

References

1. E. Hamden et al. "FIREBall-2: the faint intergalactic medium redshifted emission balloon telescope," *Astrophys. J.* **898**, 170 (2020).
2. S. E. Tuttle et al., "The FIREBall fiber-fed UV spectrograph," *Proc. SPIE* **7014**, 70141T (2008).
3. G. Kyne et al., "Delta-doped electron-multiplying CCDs for FIREBall-2," *J. Astron. Telesc. Instrum. Syst.* **6**, 011007 (2020).
4. E. T. Hamden et al., "Fireball-2: advancing TRL while doing proof-of-concept astrophysics on a suborbital platform," *Proc. SPIE* **10982**, 1098220 (2019).
5. V. Picouet et al., "End-to-end ground calibration and in-flight performance of the FIREBall-2 instrument," *J. Astron. Telesc. Instrum. Syst.* **6**, 044004 (2020).
6. M. Bass et al., *Handbook of Optics, Third Edition Volume I: Geometrical and Physical Optics, Polarized Light, Components and Instruments*, McGraw-Hill Education (2009).

Biographies of the authors are not available.